1-1-2004

Energy systematics of low-lying collective states within the framework of the interacting vector boson model

H. G. Ganev
Institute for Nuclear Research and Nuclear Energy Bulgarian Academy of Sciences

V. P. Garistov
Institute for Nuclear Research and Nuclear Energy Bulgarian Academy of Sciences

A. I. Georgieva
Institute for Nuclear Research and Nuclear Energy Bulgarian Academy of Sciences

J. P. Draayer
Louisiana State University

Recommended Citation

Ganev, H., Garistov, V., Georgieva, A., & Draayer, J. (2004). Energy systematics of low-lying collective states within the framework of the interacting vector boson model. *Physical Review C - Nuclear Physics, 70* (5) https://doi.org/10.1103/PhysRevC.70.054317

Energy Systematics of Low-lying Collective States within the Framework of the Interacting Vector Boson Model

H. G. Ganev[1], V. P. Garistov[1], A. I. Georgieva[1,2] and J. P. Draayer[2]
[1]*Institute of Nuclear Research and Nuclear Energy, Bulgarian Academy of Sciences, Sofia1784, Bulgaria*
[2]*Louisiana State University, Department of Physics and Astronomy, Baton Rouge, Louisiana, 70803-4001 USA*

In a new application of the algebraic Interacting Vector Boson Model (IVBM), we exploit the reduction of its $Sp(12,R)$ dynamical symmetry group to $Sp(4,R)\otimes SO(3)$, which defines basis states with fixed values of the angular momentum L. The relationship of the latter to $U(6)\subset U(3)\otimes U(2)$, which is the rotational limit of the model, means the energy distribution of collective states with fixed angular momentum can be studied. Results for low-lying spectra of rare-earth nuclei show that the energies of collective positive parity states with $L=0,2,4,6...$ lie on second order curves with respect to the number of collective phonons n or vector bosons $N=4n$ out of which the states are built. The analysis of this behavior leads to insight regarding the common nature of collective states, tracking vibrational as well as rotational features.

PACS numbers: 21.10.-k, 21.10.Re, 21.60.Fw, 27.70.+q

I. INTRODUCTION

A theoretical description of experimental data on the low-lying collective states of even-even nuclei in the rare-earth and actinide regions remains a problem of special interest in the nuclear structure physics. Typically data is classified from the perspective of sequences of nuclei [1], with nuclear characteristics studied as a function of the number of valence nucleons. Such results show the evolution of nuclear structure as a function of mass number, usually starting with yrast states of nuclei within a given shell [2]. But modern experimental techniques have advanced to the point that information is often available on long sequences of non-yrast in addition to yrast states with $\mathbf{J}^\pi = 0^+, 2^+, 4^+, 6^+...$ within a given nucleus [3]. In some cases the data is sufficient to justify the use of a statistical approach for studying the distribution of such states, like in shell model studies of the spacing distributions for fixed-particle-rank interactions [4]. For example, thirteen 0^+ states have been identified in ^{174}Hf [5] while in ^{168}Er five 0^+, twelve 2^+, seven 4^+ and seven 6^+ states are known. Many other such examples can be identified. Overall, theory has fallen short of being able to reproduce the rich array of experimental results.

In the more traditional quasi-particle-phonon model [6], the nature of the excited bands depends on the number of phonons and quasi-particle pairs included in the theory. Algebraic approaches, like the interacting boson model (IBM) [7] are also quite successful in understanding the behavior of the collective states, and again an important element in the analysis is the number of collective bosons used to build the states. In this regard, symplectic models provide a general framework [8] for investigating collective excitations in many-body systems as they allow for a change in the number of "elementary" excitations in the collective states. The fact that the symplectic group is also a dynamical group for the harmonic oscillator, which underpins the shell model, led to the development of very powerful symplectic shell models [8, 9] where statistical measures can be used to truncate the symplectic model spaces so that microscopic calculations are feasible [10].

Recently an empirical analysis of the data for energies of low-lying excited states in even-even nuclei was reported [11]. In the analysis, experimental energies for 0^+ excited states in the spectra of the well-deformed nuclei were classified according to the number of monopole bosons, using a simple Hamiltonian for generating a parabolic type energy spectrum [12]. Here, as in the empirical investigation cited above, we consider systematics in the behavior of the energies of sequences of collective states with a fixed angular momentum L in even-even nuclei. The energy distribution of these states with respect to the number of "elementary excitations" (phonons) that goes into their construction is best reproduced and interpreted within the framework of algebraic approaches that involve symplectic symmetries.

A description of the energies of collective states having specific L values is related to the choice of the dynamical symmetry group and its reductions. The phenomenological Interacting Vector Boson Model (IVBM) [13] has been shown to yield an accurate description of the low-lying spectra of well-deformed even-even nuclei. The most general spectrum generating algebra of the model is the algebra of the $Sp(12,R)$ group [14]. In the rotational limit [15] of the model, the reduction of $Sp(12,R)$ to the $SO(3)$ angular momentum group is carried out through the compact unitary $U(6)$ subgroup, which defines a boson-number preserving version of the theory.

In the present paper we introduce the "symplectic" reduction of $Sp(12,R)$ to the noncompact direct product $Sp(4,R)\otimes SO(3)$, which isolates sets of states with given L value (Section II). In this reduction, $Sp(4,R)$ can be

considered as a classification group for the basis states of the system [16]. To complete the labelling of the basis state, we use the reduction of irreducible representations (irreps) of $Sp(4,R)$ into irreps of the pseudo-spin group $SU(2)$ [17] (Section III). As a result of the correspondence between the symplectic and unitary reduction chains and the relation between the second order Casimir operators of $SU(3)$ and $SU(2)$, we use the same Hamiltonian and basis as in the rotational limit of the theory [14]. The eignevalues of the Hamiltonian for states with a given value of L give the energy distribution as a function of the number of excitations N that are used to build the states. The application of this new version of the IVBM (Section IV) to five even-even rare-earth nuclei confirms the empirical analysis given in [11], and extends it to include in addition to deformed nuclei, some nearly spherical ones. The analysis of the results outlines common as well as specific features of the two main types of collective motion (Conclusions).

II. GROUP THEORETICAL BACKGROUND

We consider $Sp(12,R)$, the group of linear canonical transformation in a 12-dimensional phase space [18], to be the dynamical symmetry group of the IVBM [13]. Its algebra is realized in terms of creation (annihilation) operators $u_m^+(\alpha)(u_m(\alpha) = (u_m^+(\alpha))^\dagger)$, of *two* types of bosons differing by a "pseudo-spin" projection $\alpha = \pm 1/2$ in a 3-dimensional oscillator potential $m = 0, \pm 1$. Hence the bosons that "built up" the collective excitations in the nuclear system are components of $SO(3)$ vectors and form a "pseudo-spin" doublet of the $U(2)$ group. The bilinear products of the creation and annihilation operators of the two vector bosons generate the noncompact symplectic group $Sp(12,R)$:

$$F_M^L(\alpha,\beta) = \sum_{k,m} C_{1k1m}^{LM} u_k^+(\alpha) u_m^+(\beta),$$

$$G_M^L(\alpha,\beta) = \sum_{k,m} C_{1k1m}^{LM} u_k(\alpha) u_m(\beta), \qquad (1)$$

$$A_M^L(\alpha,\beta) = \sum_{k,m} C_{1k1m}^{LM} u_k^+(\alpha) u_m(\beta),$$

where C_{1k1m}^{LM} are the usual Clebsh-Gordon coefficients and $L = 0, 1, 2$, with $M = -L, -L+1, ..., L-1, L$, define the transformation properties of (1) under rotations. Being a noncompact group, the representations of $Sp(12,R)$ are infinite dimensional. The action space of the operators (1) is in general reducible and the invariant operator $(-1)^N$, where $N = -\sqrt{3}[A^0(p,p) + A^0(n,n)]$ $(p = 1/2, n = -1/2)$ counts the total number of bosons, decomposes it into even H_+ with $N = 0, 2, 4, ...$, and odd H_- with $N = 1, 3, 5, ...$, subspaces.

A. Reduction through the compact $U(6)$

The operators $A_M^L(\alpha,\beta)$ from (1) generate the maximal compact subgroup $U(6)$ of $Sp(12,R)$. So the even and odd unitary irreducible representations (UIR) of $Sp(12,R)$ split into a countless number of symmetric UIR of $U(6)$ of the type $[N]_6 = [N, 0^5] \equiv [N]$, where $N = 0, 2, 4, ...$ for even N values and $N = 1, 3, 5, ...$ for the odd N values [17]. The rotational limit [15] of the model is further defined by the chain:

$$\begin{array}{ccccccc} U(6) & \supset & SU(3) & \times & U(2) & \supset & SO(3) \times U(1) \\ [N] & & (\lambda,\mu) & & (N,T)\ K & & L \qquad T_0 \end{array} \qquad (2)$$

where the labels below the subgroups are the quantum numbers corresponding to their irreps. In this limit, the Hamiltonian is expressed in terms of the first and second order invariant operators of different subgroups in (2). The *complete* spectrum of the system is calculated through the diagonalization of the Hamiltonian in the subspaces of *all* the UIR of $U(6)$ belonging to a given UIR of $Sp(12,R)$ [14]. Since the reduction from $U(6)$ to $SO(3)$ is carried out via the mutually complementary groups $SU(3)$ and $U(2)$ [19], their Casimir operators [17, 20, 21] as well as their quantum numbers are related to one another: $T = \frac{\lambda}{2}, N = 2\mu + \lambda$. Making use of the latter, the model Hamiltonian can be expressed as a linear combination of the first and second order Casimir invariants of the subgroups in (2):

$$H = aN + bN^2 + \alpha_3 T^2 + \beta_3 L^2 + \alpha_1 T_0^2. \qquad (3)$$

This Hamiltonian is obviously diagonal in the basis:

$$|\,[N]_6; (\lambda,\mu); K, L, M; T_0\rangle \equiv |\,(N,T); K, L, M; T_0\rangle. \quad (4)$$

B. The reduction through the noncompact $Sp(4,R)$

In the present application of IVBM we make use of another possible reduction [18] of the $Sp(12,R)$ group; namely, through its noncompact subgroup $Sp(4,R)$:

$$Sp(12,R) \supset Sp(4,R) \otimes SO(3). \qquad (5)$$

The generators of $Sp(4,R)$ are obtained from the vector addition to $L = 0$ (scalar products) of the different pairs of vector bosons $u_m^+(\alpha), (u_m(\alpha))$ $m = 0, \pm 1$ representing the $Sp(12,R)$ generators (1). By construction, all of these operators are rotational scalars and as a consequence the generators of $Sp(4,R)$ $[F^0(\alpha,\beta), G^0(\alpha,\beta)$ and $A^0(\alpha,\beta)]$ commute with components of the angular momentum, $L_M = -\sqrt{2}\sum_\alpha A_M^1(\alpha,\alpha)$, that generate the $SO(3)$ group; that is, a direct product of the two groups is realized (5). It follows from this that the quantum number L of the angular momentum group $SO(3)$ can be used to characterize the representations of $Sp(4,R)$.

The general reduction scheme of the boson representations of $Sp(4k,R)$, $k = 1, 2, ...$, to its maximal compact $U(2k)$ and noncompact $U(k,k)$ subgroups is given

in detail in [17]. The case of $k = 3$, corresponding to the reduction of $Sp(12, R)$ through the compact $U(6)$ subgroup, was presented in the symplectic extension of the $U(6)$ number conserving version of the IVBM [14]. The $Sp(4, R)$ represents the simplest nontrivial $k = 1$ case. The subgroup associated with its compact content is $U(2)$. It is generated by the Weyl generators $A^0(\alpha, \beta)$:

$$\begin{array}{l} A^0(p,n) = \sqrt{\frac{2}{3}}T_+,\ A^0(n,p) = -\sqrt{\frac{2}{3}}T_-, \\ A^0(p,p) = \sqrt{\frac{1}{3}}N_+,\ A^0(n,n) = \sqrt{\frac{1}{3}}N_-, \end{array} \tag{6}$$

where $N_+(N_-)$ count the number of particles of each kind. It is well known that $Sp(4, R)$ is very convenient for the classification [16] of nuclear properties with respect to the reduction operators $N = N_+ + N_-$ and the third projection $T_0 = -\sqrt{\frac{3}{2}}[A^0(p,p) - A^0(n,n)]$ of the pseudo-spin operator T. So we can use the equivalent set of infinitesimal operators that contain in addition to the raising T_+ and lowering T_- components of the pseudo-spin (see (6)) the Cartan operators N and T_0. The operators $T_0, T_\pm$ close the pseudo-spin algebra $su(2)$. The operator N generates $U(1)$ and plays the role of the first-order invariant of $U(2) \supset SU_T(2) \otimes U_N(1)$. So this reduces the infinite dimensional representation of $Sp(4, R)$ to an infinite sum of finite dimensional representations $[N]_2 = [N, 0] \equiv [N]$ of $U(2)$. The minimum number of bosons that are required to build a state with given L is $N_{\min} = L$ for the L even and $N_{\min} = 2L$ for the L odd. The standard labelling of the $SU_T(2)$ basis states is by means of the eigenvalues $T(T+1) = \frac{N}{2}(\frac{N}{2}+1)$ of the second order Casimir operator $\mathbf{T}^2$ of $SU(2)$. Hence $T = \frac{N}{2}, \frac{N}{2}-1, ..., 1$ or 0, for each fixed N in the reduction $Sp(4, R) \supset U(2)$. The other label of the $SU_T(2)$ basis states is provided by the eigenvalues of the operator T_0, which are $T_0 = -T$, $-T+1, \ldots, T-1, T$.

In physical applications, the following correspondence between the two chains ($U(6)$ (2) and $Sp(4, R)$ (5)) of subgroups of $Sp(12, R)$ plays an important role [22]:

$$\begin{array}{ccccc} Sp(12,R) & \supset & Sp(4,R) & \otimes & SO(3) \\ \cup & & \cup & & \cap \\ U(6) & \supset & U(2) & \otimes & SU(3). \end{array} \tag{7}$$

Result (7) is a consequence of the equivalence of the $U(2)$ group of the pseudo-spin T in both chains ($U(6) \supset SU(2) \subset Sp(4, R)$) and its complementarity to $SU(3)$ in the $SU(3) \subset U(6)$ chain.

C. Representations of $Sp(4, R)$

As noted above, each $Sp(4, R)$ irrep is infinite dimensional and consists of a countless number of $U(2)$ irreps. A basis for its representations in the even H_+ action space is generated by a consecutive application of the symmetrically coupled products of the operators $F^0(\alpha, \beta)$ to the lowest weight state (LWS) with angular momentum L that labels the $Sp(4, R)$ irrep under consideration [22, 23, 24]. Each starting $U(2)$ configuration is characterized by a totally symmetric representation $[L]$ formed by $N_{min} = L$ vector bosons. We now give a procedure for obtaining the rest of the $SU(2)$ irreps in a given L irrep of $Sp(4, R)$. To do this, we first partition r into a sum of sets (r_1, r_2) with both r_1 and r_2 even and $r_1 + r_2 = r$, where $r/2$ gives the degree of the $F^0(\alpha, \beta)$ that is applied to the LWS. These pairs can be put into one-to-one correspondence with the irreps of $U(2)$, and upon reduction to irreps of $SU(2)$ ($[r_1, r_2] \to [r_1 - r_2, 0] \equiv [r_1 - r_2]$), the decompostion is as follows: $[r] = \bigoplus_{i=0}^{\langle r/4 \rangle} [r - 4i]$, where $\langle r/4 \rangle$ denotes the integer part of the ratio. Next, the action of the various products of $F^0(\alpha, \beta)$ operators is given by all inner products of the representations $[L]$ i.e. $[L] \otimes ([r] \oplus [r-4] \oplus ...)$ restricted to two-dimensional Young diagrams. They are then transformed into $SU(2)$ representations $[k]$ corresponding to $N = N_{min} + r$, $r = 0, 2, 4, 6, ...$ and $T = \frac{k}{2} = \frac{N}{2}, \frac{N}{2} - 1, ..., 0$ for even L values. The decomposition of $Sp(4, R)$ representations for odd values of $L = 1, 3, 5$ in the even H_+ are obtained in the same way but using the decomposition of $r = 2, 4, 6, ...$ into a sum of pairs of $[r_1, r_2]$ with r_1 and r_2 both odd numbers [25] and the multiplication starting with even representations $[L-1]$. As a result of the multiplication of each given value of L with an infinite number of $SU(2)$ decompositions of the even numbers n, we obtain all the $SU(2)$ irreps contained in the $Sp(4, R)$ representation defined by L. We illustrate this technique for the cases $L = 0$ and $L = 2, 4$ in the TABLES I, II, and III. The columns are defined by the pseudo-spin quantum number $T = k/2$ and the rows by the eigenvalues of $N = k_{\max} = L + r$ for L even and $N = k_{\max} + 2 = 2L + r$ for L odd and $r = 0, 2, 4, 6, ...$ TABLE I for the $L = 0$ states actually coincides with the decomposition of the even numbers r.

The correspondence (7) between the two $Sp(12, R)$ subgroup chains, together with the relationships between the quantum numbers of $U(2)$ and $SU(3)$, allows one to identify the $SU(3)$ irreps ($\lambda = k$, $\mu = (N-k)/2$) that are shown in TABLES I, II, and III. For a given value of N, these can be compared to the classification scheme for $SU(3)$ irreps in the even $U(6)$ irreps of $Sp(12, R)$ given in TABLE I of Ref. [14]. The $SU(2)$ irreps that are missing from the tables do not contain states with the L value being considered, the latter being determined by the reduction rules for $SU(3) \supset SO(3)$ [15]. Except for the $L = 0$ case in TABLE I, in the decomposition of $Sp(4, R)$ representations L into $[k]$ irreps of $SU(2)$, there is a multiplicity in the appearance of some of the irreps. The symbol $(\rho \times)$, where ρ is an integer number, in TABLES II and III that shows how many times (ρ) the respective irrep $[k]$ appears for the specified N value. This multiplicity is exactly equal to the multiplicity of L in the reduction of the corresponding (λ, μ) irrep of

$SU(3)$ to L of $SO(3)$ [22].

TABLE I: $L = 0$

... $T=5$	$T=4$	$T=3$	$T=2$	$T=1$	$T=0$	T/N
					$[0](0,0)$	$N=0$
				$[2](2,0)$		$N=2$
			$[4](4,0)$		$[0](0,2)$	$N=4$
		$[6](6,0)$		$[2](2,2)$		$N=6$
...	$[8](8,0)$		$[4](4,2)$		$[0](0,4)$	$N=8$
$[10](10,0)$		$[6](6,2)$		$[2](2,4)$		$N=10$
...	...	...	...	...	...	...

TABLE II: $L = 2$

... $T=5$	$T=4$	$T=3$	$T=2$	$T=1$	$T=0$	T/N
				$[2](2,0)$		$N=2$
			$[4](4,0)$	$[2](2,1)$	$[0](0,2)$	$N=4$
		$[6](6,0)$	$[4](4,1)$	$2\times[2](2,2)$		$N=6$
	$[8](8,0)$	$[6](6,1)$	$2\times[4](4,2)$	$2\times[2](2,3)$	$[0](0,4)$	$N=8$
$[10](10,0)$	$[8](8,1)$	$2\times[6](6,2)$	$2\times[4](4,3)$	$2\times[2](2,4)$		$N=10$
... ...	...	...	....	...	...	...

TABLE III: $L = 4$

... $T=5$	$T=4$	$T=3$	$T=2$	$T=1$	$T=0$	T/N
			$[4](4,0)$			$N=4$
		$[6](6,0)$	$[4](4,1)$			$N=6$
	$[8](8,0)$	$[6](6,1)$	$2\times[4](4,2)$	$2\times[2](2,3)$	$[0](0,4)$	$N=8$
$[10](10,0)$	$[8](8,1)$	$2\times[6](6,2)$	$2\times[4](4,3)$	$2\times[2](2,4)$		$N=10$
... ...	...	...	....	...	...	...

III. ENERGY DISTRIBUTION OF LOW-LYING COLLECTIVE STATES

A. Application of the theory

Because of the correspondence between the symplectic and unitary reduction chains (7) and the relation between the $SU(3)$ and $SU(2)$ second order Casimir operators, in the present case we can use the same Hamiltonian (3) as in [14]. Furthermore, as established above, the bases in the two cases are equivalent and as a result the Hamiltonian (3) is diagonal in both (4). The eigenvalues for states of a given L value are therefore simply

$$E((N,T);KLM;T_0) = aN + bN^2 + \alpha_3 T(T+1) + \alpha_1 T_0^2 + \beta_3 L(L+1). \quad (8)$$

In this expression (8) the dependence of the energies of the collective states on the number of phonons (vector bosons) N is parabolic. All the rest of the quantum numbers T, T_0, and L defining the states are expressed in terms of N by means of the reduction procedure described above. This result affirms the conclusions of an empirical investigation of the behavior of states with fixed angular momentum [11], namely, that their energies are well described by the simple phenomenological formula $E_L(n) = A_L n - B_L n^2$, where $A_L > 0$ and $B_L > 0$ are fitting parameters and n is an integer number corresponding to each of the states with given L. The number n labelling each state is related in [12] to the number of monopole bosons, which are obtained by means of a Holstein-Primakoff mapping [26] of pairs of fermions confined to a j-orbit with projection m. In further considerations we have established a relation $N = 4n$ between the quantum number N and the number of ideal bosons n introduced in [12]. This relates the $Sp(12,R)$ phenomenological collective model to a simple microscopic description of the collective states.

From this analysis, it should be clear that the IVBM can be used to investigate energy distributions (8) of low-lying states with $J^\pi = 0^+, 2^+, 4^+ ...$ as a function of the number of bosons. In the applications that follow, we focus on states with $L = 0, 2, 4$. The basis states have a fixed T value the parity defined as $\pi = (-1)^T$ [14]. In the columns with fixed T, the number of bosons N changes

in steps of four ($\Delta N = 4$) in the $L = 0, 1$ cases and steps of two ($\Delta N = 2$) for all the rest (see examples given in TABLES I-III).

In what follows we present a procedure for obtaining the energy distribution of low-lying collective states in real nuclei. We start with an evaluation of the inertia parameter, β_3, that muliplies the $L(L+1)$ term in (8). This is done by fitting energies of the ground-state-band (GSB) with $L = 0_1, 2_1, 4_1, 6_1, ...$ to the experimental values for each nucleus. The other collective states in this approach, which typically are associated with other terms in the eigenvalues of the Hamiltonian (8), are also influenced by the value of the inertia parameter. A convenient method for determining the other parameters of the Hamiltonian (3) follows:

- For the 0^+ states we fix $T = 0$ and $T_0 = 0$ with $N = 0, 4, 8, ...$, which corresponds to the first column on TABLE I. As a result, we obtain a simple two-parameter quadratic equation

$$E((N_{0_i}, 0); 000; 0) = aN_{0_i} + bN_{0_i}^2 \tag{9}$$

  for the energy distributions of the $i = 1, 2, 3, ...$ experimentally observed 0_i^+ state. The index i denotes an ordering of the states with increasing energy. The $E_{0_1^+} = 0$ equation for the ground state has two solutions, namely, $N'_{0_1} = 0$ and $N''_{0_1} = -\frac{a}{b}$, as the parabola is a symmetric curve with respect to its maximum value at $N_{0_{\max}} = -\frac{a}{2b}$ for $b < 0$. The values of N_{0_i} corresponding to the experimentally observed $E_{\exp}$ and the values of the parameters a and b are evaluated in a multi-step χ-squared fitting procedure. Specifically, the fitting is performed by comparing the energies of various possible sets of values of N_{0_i} attributed to the experimental data for the 0_i^+ states. The set with minimal χ^2 value determines the distribution of the 0_i^+ states energies (a and b) with respect to the number of bosons N_{0_i} out of which each state is built.

- For 2^+ states we leave the a and b parameters fixed as determined above for 0^+ states and introduce a dependence on the quantum number $T \neq 0$ (even) and $T_0 = 0$ with allowed values of N at fixed T, $N = 2T, 2T+2, 2T+4, ...$ (third, fifth, etc., column in TABLE II). This determines the $\alpha_3 T(T+1)$ part of the Hamiltonian eigenvalue (8). In this case the α_3 parameter is again evaluated by means of a χ^2 fitting to values for the different sets of the allowed N_{2_i} attributed to the experimentally observed 2_i^+ states. This term plus the constant $6\beta_3$ fix the distance the 2^+ parabolas are separated from the 0^+ ones.

- For the 4^+ states, we again use fixed $T \neq 0$ (even) and keep the values of a, b and α_3, as determined for the 0^+ and 2^+ states, respectively, but choose $T_0 \neq 0$ from the allowed set given by $T_0 = \pm 1, \pm 2, ..., \pm T$. This choice allows one to evaluate the final parameter in the Hamiltonian, α_1. This parameter determines the distance the parabolas representing the 4_i^+ states are shifted from those previously determined, with the appropriate set of values of N_{4_i}, which gives the energy distribution of the 4^+ states with respect to N_{4_i} by means of the same type of multi-step fitting.

The model parameters are fixed with respect to the $0^+, 2^+$ and 4^+, as there is usually enough of these states to achieve good fitting statistics and they are predominantly bandhead configurations (all the 0^+ and some of the 2^+ and 4^+ states). Sets of states with other values of $L = 1, 3, 6$ or with negative parity (T-odd) can be included in the consideration by determining in a convenient way the values of T, T_0 and finding sequences of N corresponding to the observed experimental energies. Of course, the quantum numbers T, T_0 and the sequences of N have to be allowed in the reduction of the $Sp(4, R)$ representation defined by L, to the $SU(2)$ irreps. As all the parameters of Hamiltonian are evaluated from the distribution of $0^+, 2^+$ and 4^+ states, only changing the values of T and T_0 is not enough to make the curve for the additional set of states with another L distinguishable. In order to do this, we can introduce a free additive constant c_L to the eigenvalues $E((N, T); KLM; T_0)$, which is evaluated in the same way as the other parameters of (8) in a fit to the experimental values of the energies of the additional set of L states being considered.

B. Analysis of the results

The results of the treatment described above applied to the collective spectra of five even-even nuclei from the rare earth region are illustrated in Figures 1-3. The distribution of the energies with respect to values of N_{L_i} and the good agreement between theory and experiment can be clearly seen in the figures. Additionally $N_{\min}$, the values of T, T_0 used for the states with given L, the values obtained for the Hamiltonian parameters β_3, a, b, α_3, α_1 and c_L with their respective χ^2 are given in TABLE IV. The s in the first column gives the number of the experimentally observed states with the respective L value.

As already mentioned, the examples chosen for the present study consists of nuclei for which there is experimental data on low-lying energies of more than five states in each of the angular momenta $L = 0, 2, 4$ classes. Of the examples considered, two of the nuclei have typical vibrational spectra [27]: ^{144}Nd and ^{148}Sm while the rest ^{154}Gd,^{168}Er and ^{178}Hf possess typical rotational character. This is confirmed by the values obtained for the inertia parameter, β_3, given in TABLE IV. One of the main distinctions of these two types of spectra is the position of the first excited 2_1^+ state above the GSB. For vibrational nuclei the number is rather high, around

TABLE IV: Parameters of the Hamiltonian obtained in the fitting procedure

Nucleus	s	L	$N_{\min}$	T	T_0	χ^2	parameters
^{148}Sm	5	0	0	0	0	0.0005	$a = 0.03096$
							$b = -0.00010$
	7	2	8	4	0	0.0002	$\alpha_3 = -0.00187$
	10	4	6	8	8	0.0003	$\alpha_1 = -0.00285$
	3	6	20	10	10	0.0023	$\beta_3 = 0.03929$
^{144}Nd	7	0	0	0	0	0.0001	$a = 0.02389$
							$b = -0.00003$
	11	2	12	6	0	0.0008	$\alpha_3 = 0.00309$
	7	4	20	10	10	0.0004	$\alpha_1 = -0.00450$
							$\beta_3 = 0.04074$
^{168}Er	6	0	0	0	0	0.0006	$a = 0.04270$
							$b = -0.00017$
	11	2	4	2	0	0.0022	$\alpha_3 = 0.07298$
	11	4	4	2	2	0.0015	$\alpha_1 = 0.10910$
	7	3	4	2	0	0.0009	$\beta_3 = 0.01295$
							$c_3 = 0.03$
^{178}Hf	7	0	0	0	0	0.0010	$a = 0.02666$
							$b = -0.00007$
	9	2	4	2	0	0.0008	$\alpha_3 = 0.02677$
	9	4	4	2	2	0.0016	$\alpha_1 = 0.05274$
	7	6	6	2	2	0.0008	$\beta_3 = 0.01482$
^{154}Gd	11	0	0	0	0	0.0023	$a = 0.05218$
							$b = -0.00019$
	17	2	4	2	0	0.0482	$\alpha_3 = 0.0400$
	8	4	4	2	2	0.0027	$\alpha_1 = 0.09574$
	6	6	8	4	2	0.0023	$\beta_3 = 0.01634$
	3	3	4	2	0	0.0033	$c_3 = 0.05$
	2	5	6	2	0	0.00008	$c_5 = 0.09$

$1MeV$, while for the well deformed nuclei it lies at about $0.07MeV$, roughly an order of magnitude less than for the vibrational case.

For ^{144}Nd and ^{148}Sm which have vibrational spectra we apply the procedure as described above with even T values that differ considerably ($\Delta T = 4$) for the distinct sets of L values. This corresponds to rather large changes in the values of the initial $N_{min} = 2T$. Most of the states with fixed L are on the left-hand-side of the symmetric parabolas, so the values of N_{L_i} increase with an increase in the energy of these states. The step with which N_{L_i} increases depends on the energy differences between the states on the parabola. These differences are the largest for the 0^+ states and usually decrease with increasing L. This is because all of the 0^+ states are bandheads, and some of the 2^+ and 4^+ states belong to these bands. By looking at the states as distributed on the parabolas one can recognize their ordering into different bands. The GSB is formed from the lowest states with $J^\pi = 0^+, 2^+, 4^+$ is almost equidistant in the case of vibrational nuclei with very close or even equal values of n for the states in the other excited bands. The $0^+, 2^+, 4^+$ triplets of states that is almost degenerate in energy is characteristic of the harmonic quadrupole vibrations that can be observed on the theoretical energy curves, and are

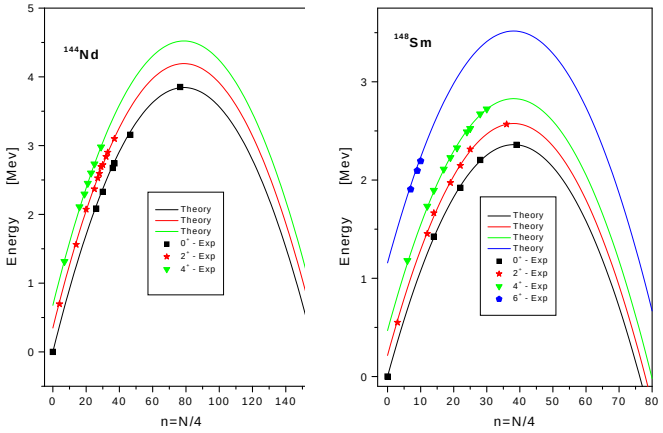

FIG. 1: (Color online) Comparison of the theoretical and experimental energy distributions of the states with $J^\pi = 0^+, 2^+, 4^+$ for ^{144}Nd (left) and with $J^\pi = 0^+, 2^+, 4^+$ and 6^+ for ^{148}Sm (right)

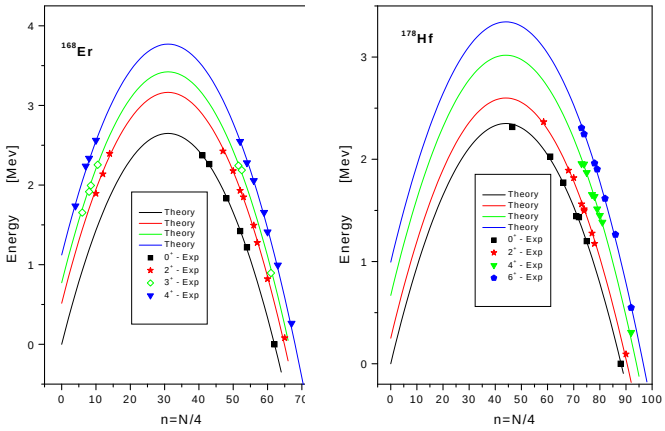

FIG. 2: (Color online) The same as in FIG.1, but for states with $J^\pi = 0^+, 2^+, 3^+\ 4^+$ in ^{168}Er (left) and $J^\pi = 0^+, 2^+, 4^+$ and 6^+ in ^{178}Hf(right)

characterized with almost equal differences between their respective values of N. A good example is observed in FIG. 1 (left) for the ^{144}Nd spectra, where such a triplet is formed by the $0_2^+, 2_3^+, 4_2^+$ states with $n = 25, 20, 15$, respectively.

The other three examples, ^{154}Gd,^{168}Er and ^{178}Hf, shown in FIGs. 2 and 3, are typical rotational nuclei. The rotational character of the spectra requires small differences in the values of N for states with $J^\pi = 0_1^+, 2_1^+, 4_1^+$ belonging to the GSB. So, for the sequences of L states being considered we have to use almost equal values of T, which corresponds to nearly equal values of $N_{\min}$. To avoid a degeneracy of the energies with respect to N_{L_i} for the nuclei with rotational spectra, and to clearly distinguish the parabolas, we have to use the symmetric feature of the second order curves. This motivates our use of the second solution $N''_{0_1} = -\frac{b}{a}$ of the equation for

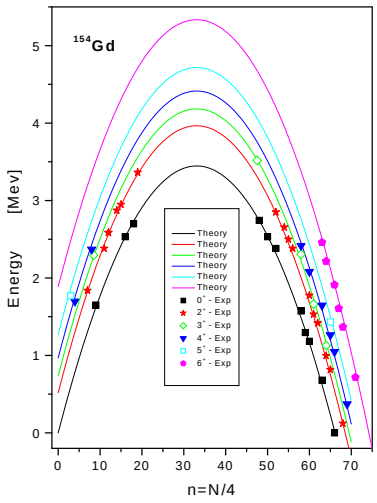

FIG. 3: (Color online) The same as in FIG.1, but for states with $L = 0^+, 2^+, 3^+, 4^+, 5^+$ and 6^+ in ^{154}Gd

the ground state (9), defining the maximum N_{0_1} for the ground state which yields a restriction on the values of N_{L_i} [10]. These increase for the $L > 0 = 2, 4, 6...$ states but not as much as in the vibrational case. Hence, it is convenient in this case to place the states with a given L in the rotational spectra on the right-hand-side of the theoretical curves. As a result, with increasing energy on a specified parabola the number of bosons that are required to build states decreases. In short, if the number of quanta required for a collective state is taken as a measure of collectivity, the states from a rotational spectra are much more collective than vibrational ones, an expected result. In this case, one can also observe the structure of collective bands that are formed by sets of states from different curves. The best examples are for the GSB and the first excited β- and γ-bands (see FIGs. 2-3). In FIG. 3, for the spectra of ^{154}Gd, in addition to the $J^\pi = 0^+, 2^+, 4^+$ states we have included states with $J^\pi = 3^+, 5^+, 6^+$. This shows that the method also works for the $K^\pi = 2^+$ and 4^+ bands. The respective values of c_L are given in TABLE IV. In this case the second 0_2^+ band is below the γ-band in contrast with the ^{168}Er and ^{178}Hf spectra [28]. The examples presented include a lot of collective states, which cannot always be clearly distinguished on the parabolas as they have almost equal values of N. For such cases the symmetry feature of the second order curves can be used to place some of them at the other side of the parabola in FIGs. 2-3.

IV. CONCLUSIONS

In this paper we introduced a theoretical framework for understanding the empirical observation that collective states fall on two parametric second order curves with respect to a variable n that counts the number of collective phonons (bosons) that is used to build the corresponding many-particle configurations.

The theory is based on the reduction of $Sp(12, R)$ into to the direct product $Sp(4, R) \otimes SO(3)$. The overarching $Sp(12, R)$ structure is the dynamical symmetry group of the Interacting Vector Boson Model (IVBM), a phenomenological model that has been shown to be successful in a description of collective nuclear states. The $SO(3)$ angular momentum group, through its role which is complementary to $Sp(4, R)$, labels states with a fixed angular momentum L. The $Sp(4, R)$ basis is obtained via a reduction of its boson representations into irreps of $SU(2)$ which are labeled by the quantum numbers T, T_0 of the pseudo-spin and its third projection. The first-order invariant of the $U(2) \subset Sp(4, R)$ is the total number of vector bosons N of the IVBM. The reduction that one exploits follows from the reduction of $Sp(12, R)$ to its maximal compact subgroup $U(6) \supset U(2) \otimes SU(3)$, which gives the rotational limit of the IVBM.

As a consequence, we use the model Hamiltonian of this limit and its eigenstates to obtain the theoretical energies of the sets of states with fixed angular momentum L. These fall on parabolas with respect to the variable $N = 4n$. The parameters of the Hamiltonian are evaluated through a fitting procedure to known experimental energies of the sets of states under consideration, that is, those with $J^\pi = 0^+, 2^+, 4^+$, and the appropriate value of N for each state. The examples presented show that the procedure is accurate and appropriate for typical collective states that are observed in atomic nuclei. In short, the theory can be applied to typical collective vibrational and rotational spectra and can be used to clearly distinguished these using symmetry properties of the second order curves. The vibrational nuclei are placed on the left-hand-side of the parabolas with differing values of T and with N increasing with increasing energies. In the rotational case the situation is the opposite, which confirms the traditional view of vibrational states as few phonon states and rotational ones that involve a higher level of collective coherence, namely, more bosons. The band structure and the energy degeneracies in both cases are also clearly observed.

The results introduced here to illustrate the theory demonstrate that the IVBM can be used to reproduce reliably empirical observations of the energy distribution of collective states. Such a demonstration can be provided for any collective model that includes one- and two-body interactions in the Hamiltonian. The main feature that leads to our parameterization is the symplectic dynamical symmetry of the IVBM. This allows for a change in the number of "phonons" that are required to build the states. This investigation also provides insight into the structure of collective states, revealing the similar origin of vibrational and rotational spectra, but at the same time yielding information about unique features that distinguish the two cases.

Acknowledgments

Support from the U.S. National Science Foundation, Grant No. PHY-0140300, is acknowledged. The authors are grateful to Dr. C. Bahri, Prof. D. Rowe and N. V. Zamfir for the helpful and enlightening discussions.

[1] R. F. Casten and N. V. Zamfir, J. Phys. G: Nucl. Part. Phys. 22 (1996) 1521.
[2] S. Drenska, A. Georgieva, V. Gueorguiev, R. Roussev and P. Raychev, Phys. Rev. C 52 (1995) 1853.
[3] Mitsuo Sacai, Atomic Data and Nuclear Data Tables 31 (1984), 399; Level Retrieval Parameters http://iaeand.iaea.or.at/nudat/levform.html
[4] S. S. M. Wong and J.B. French, Nucl. Phys. A198 (1972) 188; J.B. French and S. S. M. Wong, Phys. Lett. 35B (1971) 5.
[5] S. R. Lesher et al., Phys. Rev. **C 66** (2004) 051305(R).
[6] V. G. Soloviev, A. V. Sushkov and N. Yu. Shirikova, Progr. Part. Nucl. Phys., **27**, 667 (1996); Phys. Rev. **C 51** (1995) 551.
[7] F. Iachello and A. Arima, *"The Interacting Boson Model"*, Cambridge University Press, Cambridge, 1987.
[8] D. J. Rowe, Rep. Prog. Phys. **48** (1985) 1419.
[9] O. Castanos and J. P. Draayer, Nucl. Phys. **A491** (1989) 349.
[10] J. P. Draayer and J. Rosensteel, Phys. Lett. **124B** (1983) 281; G. Rosensteel and J. P. Draayer, Nucl. Phys. **A436** (1985) 445.
[11] V. Garistov, *Rearrangement of the Experimental Data of Low Lying Collective Excited States,* Proceedings of the XXII International Workshop on Nuclear Theory, ed. V. Nikolaev, Heron Press Science Series, Sofia (2003) 305.
[12] V. Garistov, On Description of the Yrast Lines in IBM-1, Proceedings of the XXI International Workshop on Nuclear Theory, Rila Mountains, ed. V. Nikolaev, Heron Press Science Series, Sofia (2002).
[13] A. Georgieva, P. Raychev and R. Roussev, J. Phys. G: Nucl. Phys. **8** (1982) 1377.
[14] H. Ganev, V. Garistov and A. Georgieva, Phys. Rev. **C 69** (2004) 014305.
[15] A. Georgieva, P. Raychev and R. Roussev, J. Phys. G: Nucl. Phys. **9** (1983) 521.
[16] A. Georgieva, M. Ivanov, P. Raychev and R. Roussev, Int. J. Theor. Phys. **28** (1989) 769.
[17] A. Georgieva, M. Ivanov, P. Raychev and R. Roussev, Int. J. Theor. Phys. **25** (1986) 1181.
[18] M. Moshinsky and C. Quesne, J. Math. Phys. **12** (1971) 1772.
[19] C. Quesne, J. Phys. **A18** (1985) 2675.
[20] M. Moshinsky, Rev. of Mod. Phys. **34** (1962) 813.
[21] M. Moshinsky and C. Quesne, J. Math. Phys. **11** (1970) 1631.
[22] V. V. Vanagas, *Algebraic foundations of microscopic nuclear theory,* Nauka, Moscow, (in russian) (1988).
[23] J. Escher and A. Leviatan, Phys. Rev. Lett. **84** (2000) 1866.
[24] G. Rosensteel and D. J. Rowe, Phys. Rev. Lett. **38** (1977) 10.
[25] J. P. Draayer, A. I. Georgieva and M. I. Ivanov, J. Phys. A: Math. Gen. **34** (2001) 2999.
[26] T. Holstein and H. Primakoff, Phys. Rev. **58** (1940) 1098; A. Klein and E. Marshalek, Rev. Mod. Phys. **63** (1991) 375.
[27] R. K. Sheline, Rev. Mod. Phys. **32** (1960) 1.
[28] A. Aprahamian, Phys. Rev. **C 65** (2002) 031301(R).